Cell Communication and Signaling

RESEARCH

Open Access

Helicobacter pylori infection promotes M1 macrophage polarization and gastric inflammation by activation of NLRP3 inflammasome via TNF/TNFR1 axis

Xiao Fei[1†], Sihai Chen[1,2†], Leyan Li[1], Xinbo Xu[1], Huan Wang[1,2], Huajing Ke[1], Cong He[1], Chuan Xie[1], Xidong Wu[3], Jianping Liu[1], Yong Xie[1], Nonghua Lu[1], Yin Zhu[1*] and Nianshuang Li[1*]

Abstract

Background Macrophages play a crucial role in chronic gastritis induced by the pathogenic *Helicobacter pylori* (*H. pylori*) infection. NLRP3 inflammasome has emerged as an important component of inflammatory processes. However, the molecular mechanism by which *H. pylori* infection drives NLRP3 inflammasome and macrophages activation remains unclear.

Methods Human gastritis tissues were collected for clinical significance of NLRP3. Infection with *H. pylori* was performed using in vitro and in vivo models. Bone marrow-derived macrophages (BMDMs) from wild-type (WT), *Nlrp3*-knockout (KO) and *Tnfr1*-KO mice were infected with *H. pylori*. Western blotting, qRT-PCR, immunofluorescence, immunohistochemistry and ELISA were utilized for functional and mechanistic studies.

Results Single-cell RNA sequencing (ScRNA-seq) analysis of human gastric tissues, followed by validation, indicated that NLRP3 was primarily expressed in myeloid cells and was significantly increased in *H. pylori*-positive gastritis compared to *H. pylori*-negative gastritis. Infection with PMSS1 and NCTC11637 *H. pylori* strains induced NLRP3 inflammasome activation in vitro (THP1 cells) and in the insulin-gastrin (INS-GAS) transgenic mouse model. Deletion of NLRP3 in BMDMs showed marked inhibition of *H. pylori*-induced M1 macrophage polarization. Furthermore, NLRP3 inflammasome activation upon TNFα, or *H. pylori* stimulation, was partially blocked by TNFα/TNFR1 signaling inhibitors. Deletion of TNFR1 in BMDMs significantly impaired NLRP3 inflammasome activation and M1 macrophages induced by *H. pylori*.

Conclusion This study revealed that the activation of NLRP3 inflammasome, regulated by the TNF/TNFR1 signaling axis, is a key regulator of *H. pylori*-induced M1 macrophage activation and gastritis.

Keywords *H. pylori*, NLRP3 inflammasome, TNF/TNFR1 axis, Macrophage, Gastritis

†Xiao Fei and Sihai Chen contributed equally to this work.

*Correspondence:
Yin Zhu
ndyfy01977@ncu.edu.cn
Nianshuang Li
ndyfy05390@ncu.edu.cn
Full list of author information is available at the end of the article

Introduction

Helicobacter pylori (*H. pylori*), a gram-negative bacterium that colonizes the gastric mucosa, is well known to be the main cause of gastrointestinal pathologies such as gastritis, peptic ulcers, and gastric adenocarcinoma [1, 2]. Chronic inflammation of gastric epithelium induced by bacterial pathogens is a necessary step of gastric carcinogenesis. *H. pylori* infects nearly half of the global population, with strong differences between geographical areas [3]. Most infected individuals are generally asymptomatic, however, chronic gastritis develops in all infected subjects [4]. Some individuals with *H. pylori* infection potentially develop from gastric metaplasia, dysplasia, eventually to gastric carcinoma [5, 6]. The pathogenic virulence factors cytotoxin-associated gene (CagA) and vacuolating toxin A (VacA) have been recognized to play an important role in the development of *H. pylori*-related gastric disorders [7]. Accumulating clinical evidence indicates that *H. pylori* eradication therapy based on the combined use of antibiotics and proton pump inhibitor significantly reduces the risk of developing gastric cancer [8, 9]. However, for a subset of the infected population, the benefits of *H. pylori* eradication therapy are greatly reduced due to persistent inflammation and even precancerous lesions caused by *H. pylori* infection [10]. Exploring the underlying molecular mechanism of *H. pylori*-induced gastric mucosal inflammation could provide alternative therapeutic strategies to improve the outcomes in the infected populations.

Macrophages, as a central component of the innate immune system and the first line of host defense against microbial pathogens, plays a crucial role in controlling the inflammatory response caused by *H. pylori* [11]. Macrophages typically exhibit two distinct functional phenotypes: M1 or M2 polarized macrophages. M1 macrophages, also known as classically activated macrophages, are characterized by the expression of inducible nitric oxide synthase (iNOS) expression, and increased production of pro-inflammatory cytokines or chemokines including tumor necrosis factor α (TNFα), interleukin 1 β (IL1β), interleukin 6 (IL6), chemokine Ligand 2 (CCL2), and chemokine ligand 3 (CCL3) [12]. M2 macrophages, representing anti-inflammatory response and wound repair, are marked by increased production of various cytokines including interleukin 4 (IL4), interleukin 10 (IL10), and transforming growth factor β (TGF-β) [13]. Recent studies have shown that M1 macrophage polarization in response to *H. pylori* infection is a critical step in mediating antimicrobial activity and pro-inflammatory response [14, 15]. It has been reported that the elimination of macrophages in mice reduced gastric pathology caused by *H. pylori* infection, suggesting that the importance of macrophages in the severity of *H. pylori*-triggered gastric inflammation severity [16].

The NLRP3 inflammasome is a multiprotein complex comprised of the sensor NLRP3, the adaptor ASC and the effector caspase-1 [17]. It can be activated by specific pathogens, host cellular damage, and various environmental stimuli. Assembly of the NLRP3 inflammasome leads to the maturation and release of the proinflammatory cytokines such as IL-1β and IL-18 [18]. Excessive production of IL-1β has been associated with NLRP3 inflammasome activation and linked to various inflammatory diseases, such as rheumatoid arthritis, asthma, and atherosclerosis [19]. Our recent study has identified a critical role of the NLRP3 inflammasome in the development of acute pancreatitis by modulating the gut microbiota [20]. NLRP3 is highly expressed in monocytes and macrophages [21, 22]. There is mounting evidence that *H. pylori* infection activates NLRP3 inflammasome, thereby promoting the release of IL-1β [23–25]. In murine macrophages, Toll-like receptors (TLRs) has been found to activate NLRP3 inflammasome transcriptional activation through the NF-κB pathway [26] However, the potential role of NLRP3 in macrophage polarization and the mechanisms regulating NLRP3 inflammasome activation by *H. pylori* remain poorly understood.

Tumor necrosis factor (TNF; TNFα) is constitutively expressed in multiple cell types, mostly in immune cells [27]. TNF exists in two forms: membrane-bound TNF and soluble TNF. TNF signaling occurs through two distinct receptors, TNF receptor-1 (TNFR1) and TNF receptor-2 (TNFR2). TNFR1 can be efficiently activated by both the membrane-bound and soluble forms, while TNFR2 exhibits a higher affinity for membrane-bound TNF [28]. The differences in intracellular region of the TNF receptors contributes to their distinct physiological roles [29]. As one of the most important cytokines, the primary role of TNF is the regulation of immune and inflammatory response. Most biological functions such as cell death and pro-inflammatory response regarding TNF signaling are primarily induced by TNFR1, while the role of TNFR2 is still relatively unknown [30]. It has been widely recognized that the binding of TNF ligand to TNFR1 triggers receptor trimerization, leading to the recruitment of adaptors, such as receptor interacting protein 1 (RIPK1) and TNF receptor-associated death domain (TRADD) to TNFR1. This binding ultimately results in the activation of NF-κB and MAPK signaling pathways [31].

In this study, we highlighted the crucial role of NLRP3 inflammasome in the activation of M1 macrophage and gastritis disease due to *H. pylori* infection. We found that NLRP3, which is primarily expressed in myeloid cells, had higher expression levels in *H. pylori*-infected gastritis

tissues than in non-infected tissues. We also observed that the deficiency of NLRP3 in BMDMs significantly suppressed M1 macrophages and the production of pro-inflammatory cytokines by *H. pylori*. Furthermore, we demonstrate the essential role of TNF-TNFR1 signaling in *H. pylori*-triggered NLRP3 inflammasome activation. Overall, this study has revealed a novel regulatory mechanism of TNF/TNFR1-mediated NLRP3 inflammasome, which controls M1 macrophages activation and promotes gastritis in response to *H. pylori* infection.

Materials and methods

Human clinical specimens

Thirty specimens of human gastric tissue specimens were collected from patients undergoing endoscopy and biopsy at the First Affiliated Hospital of Nanchang University in Jiangxi, China. The clinicopathological characteristics of patients were listed in Table S1. The *H. pylori* infection status of these clinical specimens was determined by the urea breath test (UBT) or immunohistochemistry. Based on *H. pylori* infection status, the specimens were divided into two subgroups: *H. pylori*-positive ($n=15$) and *H. pylori*-negative ($n=15$). The study protocol and informed consent waiver were approved by the Ethics Committee of the First Affiliated Hospital of Nanchang University ((2023) CDYFYYLK (02–012).

Mice

All procedures performed on the animals were approved by the Animal Care and Ethics Committee (CDYFY-IACUC-202302QR004) of the First Affiliated Hospital of Nanchang University. The male wild-type (WT), and *Tnfr1*-KO mice aged 6 to 8 weeks were obtained from GemPharmatech Company (Nanjing, China). The male transgenic hypergastrinemic insulin-gastrin (INS-GAS) mice (#018149), aged 6–8 weeks old and on a FVB/N background, and *Nlrp3*-knockout (KO) mice (#021302) were purchased from The Jackson Laboratory and housed under a 12-h light/dark cycle with ad libitum access to food and water. The genotyping of mice was performed according to the manufacturer's instructions. The primers used in this process are listed in Table S2. The experimental environment was maintained at a temperature of 18–26 °C and a relative humidity of 40–70%. The INS-GAS mice were infected with the mouse-adapted wild-type *H. pylori* strain PMSS1 ($2\times10\text{^}9$ CFU/mouse) via gavage every other day for a total of five times [6, 32]. Mice were orogastrically challenged with Brucella broth (BB) as a control. Mice were fasted for 4 h before and after each gavage. Mice were euthanized 16 weeks post-infection.

Isolation of bone marrow-derived macrophages (BMDMs) and cell culture

THP-1 cells were cultured in a specialized medium (RPMI-1640 medium supplemented with 10% FBS, 0.05 mM β-mercaptoethanol, and 1% P/S (Procell, Wuhan, China)). Before experimentation, the THP-1 cells were induced to differentiate into macrophages by treatment with 200 ng/ml phorbol 12-myristate 13-acetate (PMA) (MedChemExpress, HY-18739) for 48 h.

BMDMs were isolated from the femurs and tibias of WT, *Nlrp3*-KO, and *Tnfr1*-KO mice. The BMDMs suspension was obtained by flushing the bones with PBS containing 2% FBS (Gibco, Australia) and filtered through a sterile 70 μm cell strainer. After a 10-min incubation with red blood cell lysis buffer (Absin, Shanghai, China) to lyse red blood cells, cells were cultured in complete medium (RPMI-1640 supplemented with 10% FBS, 100 U/ml penicillin/streptomycin (NCM Biotech, Suzhou, China), and 100 ng/ml recombinant murine M-CSF (PeproTech, USA)) for 7 days. All cells were maintained in a humidified atmosphere at 37 °C with 5% CO_2.

Reagents and transfection

Recombinant murine M-CSF (#315–02), recombinant murine TNF-α (#315-01A), and recombinant human TNF-α (#300-01A) were purchased from PeproTech (NJ, USA). Atrosab (#HY-P990008), Nigericin (#HY-127019) and LPS (#HY-D1056) were obtained from MedChemExpress (Shanghai, China), and QNZ (#S4902) was purchased from Selleck Chemicals (HOU, USA).

Control siRNA and NLRP3 siRNA were produced by Hitrobio (Beijing, China), and then transfected into THP-1 cells using lipofectamine 3000 (Thermo Scientific, MA, USA) according to the manufacturer's instructions. The target sequences of NLRP3 siRNA were: Sense:5′-GGAGAGACCUUUAUUGAGAATT-3′; Antisense:5′-UUCUCAUAAAGGUCUCUCCTT-3′. 48 h post-transfection, cells were treated with inhibitors of the TNF/TNFR1 signaling, 1 μM Atrosab or 400 ng/ml QNZ. Western blots and qRT-PCR analysis validated the transfection efficiency.

H. pylori strains and culture

This study employed wild-type $CagA^+$*H. pylori* strains (PMSS1, NCTC11637 and 26695) [6, 33]. Isogenic PMSS1 $CagA^-$ mutant was constructed in our previous study [34]. The *H. pylori* isogenic 26695 $VacA^-$ mutant was kindly provided by Dr. Chunhui Lan from Daping Hospital, Third Military Medical University (Chongqing, China). Additionally, the rodent-adapted $CagA^+$*H. pylori* strain pre-murine Sydney Strain 1 (PMSS1) was used for animal experiments. *H. pylori* were cultured under

microaerophilic conditions on Brucella agar (BD Bioscience) supplemented with 5% sheep blood for in vitro passage. For in vitro co-culture with THP-1 cells, *H. pylori* were grown overnight in Brucella broth (BD Bioscience) supplemented with 10% FBS (Gibco, Australia). The bacteria were harvested and determined the density at 600 nm (1OD600 = 10^9 CFU/ml), then resuspended and added to THP1 or BMDM cells. Before co-culture with bacteria, each well was seeded with 1 × 10^6 cells. The bacteria were co-cultured with THP1 or BMDM cells at various multiplicities of infection (MOI = 0, 25, 50, 100 and 200) for different durations (0 h, 3 h, 6 h, 12 h and 24 h).

Assessment of *H. pylori* colonization and histopathology in gastric tissues of mouse models

The mouse stomach was opened along the greater curvature, and a linear strip of gastric tissue extending from the squamocolumnar junction to the proximal duodenum was selected. After fixation in formalin for 24 h, the tissue was dehydrated and then embedded in paraffin. Once cooled and solidified, the tissue was sectioned into approximately 4 μm thick gastric tissue slices. *H. pylori* colonization was visualized by silver staining using the Spirochete Silver Staining Kit (Warthin-Starry Method, #G1940, Solarbio Biotech, China) according to manufacturer's instructions. All images were captured using a Nikon Eclipse microscope. Additionally, the bacterial burden was calculated by determining the number of CFU per gram of tissue. In brief, the isolated gastric tissues were weighed and homogenized, then plated in brucellar broth agar plates containing 5% sheep blood, vancomycin, trimethoprim, amphotericin and polymyxin for selective *H. pylori* growth. These plates were incubated under microaerophilic conditions at 37℃ for 3–5 days, followed by the calculation of bacterial burden.

The paraffin sections were stained with Hematoxylin and Eosin (H&E). A pathologist, blinded to sample identification, evaluated the degree of inflammation and the incidence of gastric injury, including atrophy and metaplasia [35]. Alcian blue coupled with periodic acid-Schiff (AB-PAS) staining was performed to identify the type of metaplasia present, following the manufacturer's instructions (#G1285, Solarbio Biotech, China). In brief, after deparaffinization, the slides were stained with Alcian blue for 20 min, followed by oxidation and stained with Shiff reagent for 10 min. Then the slides were rinsed with running water and further stained with hematoxylin. All images were captured on a Nikon Eclipse microscope.

Immunohistochemistry

Immunohistochemical staining was conducted as previously described [6]. Briefly, the sections were sequentially soaked in xylene, 100%, 95% and 85% ethanol to remove paraffin. Antigen retrieval was then performed using sodium citrate buffer. Endogenous peroxidase activity was blocked with 3% hydrogen peroxide. Non-specific binding of antibodies was avoided by incubation in 1% BSA blocking solution for 30 min. Next, the sections were incubated with the primary antibody was incubated at 4 °C overnight, followed by 3 times wash with PBS and subsequent incubation with the secondary antibody (PV-6000, Zhongshan Biotech, China) was incubated with the sections at 37 °C for 1 h. The isotype control antibody (#3900, Cell Signaling Technology, USA) was used as a negative control to determine any nonspecific background staining (Fig. S1A). Diaminobenzidine (DAB) (ZLI-9017, Zhongshan Biotech, China) was used for color development, followed by counterstaining with hematoxylin (L25050202, YULU, China). Immunohistochemical staining was assessed by two pathologists, who were blinded to the sample identities, to determine the expression profile of NLRP3. The intensity (scored 0–3) and frequency (scored 0–4) of NLRP3 expression were evaluated and graded. In statistical analyses, the expression level of NLRP3 protein was represented by an expression score, ranging from 0 to 12, calculated as the product of intensity and frequency. All images were captured using a microscope (Nikon Eclipse).

Single-cell RNA sequencing (scRNA-seq) analysis

In our previous work [36], we included 18 patients diagnosed with gastric lesions at the First Affiliated Hospital of Nanchang University. This cohort consisted of 6 cases of gastritis (GS), 6 cases of intestinal metaplasia (IM), and 6 cases of gastric cancer (GC). The GS and IM samples were collected via endoscopy, while the GC samples were obtained from surgical specimens of patients who had not received any adjuvant therapy. Patients with gastric mucosal lesions were divided into *H. pylori-* positive and *H. pylori-* negative groups based on their infection status. The study protocol was approved by the Ethics Committee of the First Affiliated Hospital of Nanchang University, with approval number (2023) CDYFYYLK (01–009). All tissue samples were obtained with informed consent. Tissues from different stages of gastric mucosal lesions were isolated and subsequently prepared into single-cell suspensions. Libraries were prepared using the Chromium Next GEM Single Cell 3′ Reagent Kits v3.1 (Cat#1000268, 10 × Genomics) according to the manufacturer's protocol. The libraries were sequenced on the Illumina NovaSeq 6000 platform. Raw reads were processed into gene expression matrices using Cell Ranger software (10 × Genomics), followed by further quality control was performed using the Seurat package. The raw single-cell sequencing data of 18 human gastric samples from this

study have been deposited in the gene expression omnibus database (GEO), under accession code GSE249874 (https://www.ncbi.nlm.nih.gov/geo/query/acc.cgi).

The UMAP plots illustrate the expression of several genes, such as NLRP3, TNF, ASC, and IL1B, across various different cell types. To examine identify the activity of inflammasome pathway, we selected the crucial genes within this pathway, including HMOX1, MEFV, NFKB1, NFKB2, NLRC4, NLRP1, NLRP3, P2RX7 and PYCARD. Using the AddModuleScore function, we calculated the mean expression level of these genes in each cell. All figure visualizations were generated utilizing the SCP (Version 0.5.6) R package.

To analyze cell–cell interaction [37], we applied the CellChat R package to compare significant ligand-receptor pairs between *H. pylori* -positive and *H. pylori* -negative samples. During this procedure, we employed the netVisual_heatmap function to visualize variations in the number or strength of cell–cell interactions. The rankNet function was deployed to infer and rank the differences in information flow between signaling networks in gastric tissues, both *H. pylori*-infected and uninfected. The netAnalysis_contribution function was used to assess the contribution of all ligand-receptor pairs within a specific signaling network.

Western blotting

Western blotting analysis was performed according to previously describe methods [38]. Briefly, proteins were extracted using protein lysis buffer (Solarbio, Beijing, China) supplemented with phosphatase and protease inhibitors, and the protein concentrations were determined using a BCA assay kit (Thermo Scientific, MA, USA). Equal amounts of protein extracts were separated by SDS-PAGE and transferred onto nitrocellulose membranes (PerkinElmer, Waltham, MA), which were subsequently blocked with a 5% non-fat milk blocking solution. The membranes were then incubated with specific primary antibody at 4 °C overnight, followed by incubation with corresponding secondary antibodies (Invitrogen, CA, USA) for 1 h at room temperature. The Western blot immunoreactive signals were visualized using the BIO-RAD ChemiDoc XRS + system with SuperSignal West Pico stable peroxide solution (Thermo Scientific, MA, USA) in a darkroom. The specific information for primary antibodies is as follows: anti-NLRP3 (#15101S), anti-Caspase-1 (#83383), anti-Cleaved Caspase-1 (#89332, #4199), anti-IL-1β (#12242), anti-Cleaved -IL-1β (#83186), anti-NF-kB p65 (#8242), anti-Phospho-NF-κB p65 (#3033) antibodies were purchased from Cell Signaling Technology (Danvers, MA, USA). Anti-IL-6 (ab233706) was obtained from Abcam (Boston, MA, USA). Anti-TNF-α (A0277) and anti-TNFR1 (A1540) were from ABclonal Technology (Wuhan, China). Anti-STAT3 and anti-Phospho-STAT3 (Tyr705) were from Zen BioScience (Chengdu, China). Anti-β-actin (#HC201-01) was obtained from TransGen Biotech (Beijing, China), and anti-GAPDH (#10494–1–AP) was from Proteintech (Wuhan, China). All primary antibodies were used at a dilution of 1:1000, except for internal control antibodies such as GAPDH and β-actin, which were diluted at 1:2000 and 1:5000, respectively.

Immunofluorescence assay

For cell immunofluorescence staining, cells were washed with PBS at room temperature, followed by fixation with 4% formaldehyde in PBS for 30 min. Permeabilization of fixed cells was achieved using 0.3% Triton-100 for 15 min. After blocking with 3% bovine serum albumin (BSA) for 1 h, cells were incubated with primary antibodies or isotype antibody at 4 °C overnight, followed by incubation with secondary antibodies, Alexa Fluor Plus 488 or Alexa Fluor Plus 555 (1:500, Thermo Fisher, Weston, FL), in the dark for 1 h. Nuclei were counterstained with DAPI (P0131, Beyotime, China). All images were acquired using a confocal fluorescence microscope (Leica Stellaris 5). The primary antibodies used is as follows: anti-NLRP3 (Servicebio, GB114320-100, 1:200), anti-F4/80 (Servicebio, GB113373-100, 1:500), anti-CD68 (Santa Cruze, SC-20060, 1:50), anti-iNOS (Zen BioScience, 340668, 1:50) and anti-TNF-α (ABclonal, A0277, 1:50).

Quantitative real-time PCR analysis

Total RNA from cells or tissues was extracted using TRIzol (Invitrogen, CA, USA), followed by cDNA synthesis using the FastKing cDNA First Strand Synthesis Kit (KR116, Tiangen, China). SYBR® Premix Ex Taq (RR820B, TaKaRa, Japan) was used for RT-PCR analysis. mRNA levels were detected using the QuantStudio 5 Real-Time PCR System (Life Technologies). Gene-specific primers were obtained from the public database PrimerBank (Table S3).

ELISA assay

The ELISA kits for detecting the concentrations of IL-1β, TNF-α and IL-18 were purchased from Elabscience (Wuhan, China). The mouse *H. pylori* IgG antibody ELISA kit was purchased from mlbio (Shanghai, China). ELISA assay was carried out following the manufacturer's instructions. Briefly, standards or samples was added to the antibody-coated plate and incubated for 1 h at 37℃. Then the biotinylated antibody solution, avidin-HRP solution and substrate solution were added to the microplate well. The absorbance value at 450 nm was measured after the addition of the stop solution. A standard curve was drawn according to the absorbance of standards at

different concentration gradients. The concentration of cytokines in the samples was sequentially calculated using this standard curve.

Statistical analyses

All statistical analyses were performed using SPSS 21.0 software. Data are presented as means ± standard deviation (SD) from three independent experiments. Differences between the two groups were compared using Student's t-test. One-way analysis of variance (ANOVA) was used to compare statistical differences among three or more groups. Differences were considered statistically significant at $p < 0.05$(****, P < 0.001; **, P < 0.01; *, P < 0.05*).

Results

NLRP3 is primarily expressed in myeloid cells, and is significantly increased in *H. pylori*-positive gastritis tissues

In our previous work, we conducted scRNA-seq on 18 human gastric tissues including those with *H. pylori*-positive and -negative gastritis, intestinal metaplasia and gastric cancer tissues [36]. The raw sequencing data was deposited in the GEO database (GSE249874). A total of 8 cell types were identified, including gastric epithelial cells, fibroblasts, endothelial cells, smooth muscle cells, T cells, B cells, plasma cells and myeloid cells. Notably, the UMAP plot and violin plot indicated that NLRP3, the critical molecule in the initiate immune system, was primarily expressed in myeloid cells (Fig. 1A). The expression of NLRP3 was significantly higher in *H. pylori*-positive gastritis tissues compared to *H. pylori*-negative subjects (*5.17% VS 2.02%*) (Fig. 1B). To validate these findings, we performed immunofluorescence staining for co-localization of NLRP3 and CD68 (pan macrophage marker) using human gastritis tissues with or without *H. pylori* infection. Our data showed NLRP3 was expressed in $CD68^+$ macrophages and upregulated in *H. pylori*-infected gastritis tissues (Fig. 1C). In addition, western blotting analysis of human tissues showed higher levels of NLRP3 protein in *H. pylori*-infected gastritis tissue samples than in *H. pylori*-negative counterparts (Fig. 1D). These data were further confirmed by immunohistochemistry analysis, which showed significant overexpression of NLRP3 in *H. pylori*-infected gastritis tissues (Fig. 1E, F). Taken together, these findings demonstrate that NLRP3 is predominantly expressed in myeloid cells and is significantly elevated in *H. pylori*-infected human gastritis tissues.

H. pylori infection promotes NLRP3 inflammasome activation in macrophage

The interaction of NLRP3 with the adaptor ASC (also known as PYCARD) initiates inflammasome assembly, further resulting in the release of pro-inflammatory cytokines IL1β and IL18 [18]. Through analyzing the scRNA-seq data [36], we found that the inflammasome pathway (*64.35%* VS *59.61%*, Fig. S1B), including the key genes *ASC* (*32.24%* VS *25.98%*, Fig. S1C) and *IL1B* (*10.16%* VS *2.19%*, Fig. S1D), were enhanced in *H. pylori*-positive tissues, compared to negative tissues. Notably, this trend was particularly prominent in myeloid cells (Fig. S1B-D). To assess the influence of *H. pylori* on NLRP3 inflammasome in macrophages, we infected THP1 cells with *H. pylori* PMSS1 strain or NCTC11637 strain. ELISA analysis showed that IL1β secretion was increased in the supernatant of THP1 cells following *H. pylori* infection, and this occurred in dose- (Fig. 2A) and time-dependent (Fig. 2B) manners. Meanwhile, *H. pylori* infection significantly increased secretion of IL18 in THP1 cells (Fig. 2C). Additionally, western blot analysis indicated that stimulation with *H. pylori* PMSS1 strain significantly upregulated the protein expression of NLRP3, pro-IL-1β and its cleavage in a dose-dependent manner in macrophages (Fig. 2D and Fig. S2A). Similar results were achieved in cells following infection with *H. pylori* NCTC116737 (Fig. 2E and Fig. S2B). Treatment with LPS and nigericin was used as a positive control to stimulate the activation of the NLRP3 inflammasome signaling in THP1 cells (Fig. S2C). Moreover, the expression of NLRP3 and IL-1β began to increase at 3 h post-infection and progressively increases over time (Fig. 2F and Fig. S2D-E). The upregulation of NLRP3 in macrophages after infection was further confirmed via immunofluorescence staining (Fig. 2G). The formation of ASC specks was markedly increased following *H. pylori* infection (Fig. 2H).

(See figure on next page.)

Fig. 1 NLRP3 is mainly expressed in myeloid cells, and is significantly increased in *H. pylori*-positive gastritis than in *H. pylori*-negative gastritis. **A** ScRNA-seq analysis of human gastritis, intestinal metaplasia, and gastric cancer tissues was carried out in our previous studies, with raw sequencing data made available in the GEO database (GSE249874). The UMAP plot (left panel) and violin plot (right panel) showing the expression of NLRP3 in different cell populations. **B** The UMAP plots showing the expression of NLRP3 in *H. pylori*-positive and -negative gastritis tissues, respectively. **C** Immunofluorescence staining for CD68 (green) and NLRP3 (red) in human gastritis specimens with or without *H. pylori* infection. Scale bar, 10 μm. **D** Western blotting analysis for NLRP3 expression in *H. pylori*-infected and uninfected gastritis tissues. **E**, **F** Immunohistochemistry staining for NLRP3 expression in human gastritis tissues with or without *H. pylori* infection ($n = 15$ for each group). Representative images (**E**) and histological scores (**F**) were shown respectively. Scale bar, 10 μm. **, P < 0.05; **, P < 0.01; ***, P < 0.001*. Data are expressed as the means ± SDs

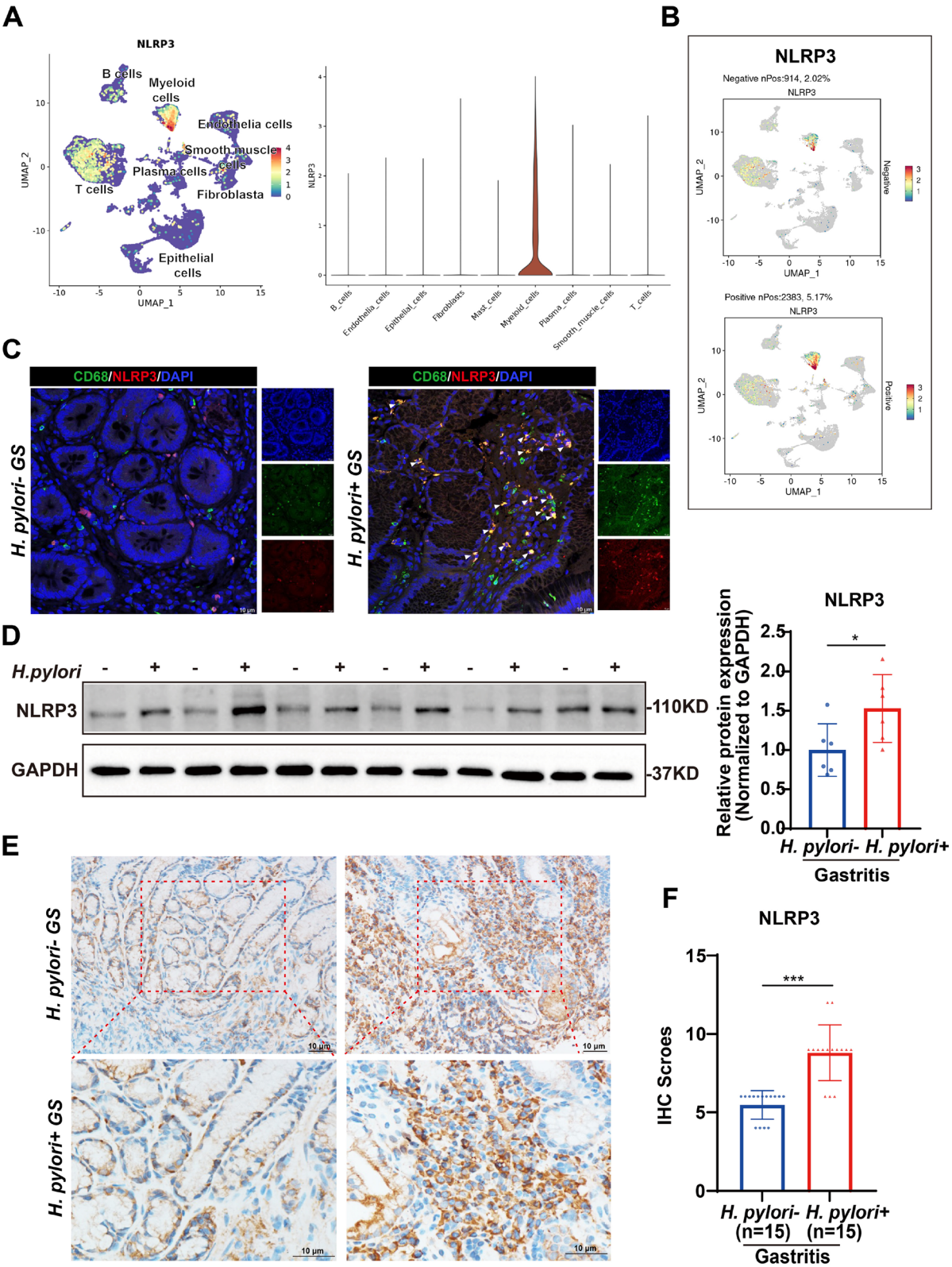

Fig. 1 (See legend on previous page.)

As bacterial proteins CagA and VacA significantly determine host-microbe interactions, we next investigate whether the induction of NLRP3 inflammasome by *H. pylori* is dependent on the virulence factors CagA or VacA by analyzing the expression of NLRP3 inflammasome proteins in THP1 cells cocultured with WT *H. pylori* PMSS1 and its $CagA^-$ isogenic mutant [34], respectively. As a result, we found that the deletion of CagA appears to not affect the regulation of NLRP3 by the PMSS1 strain (Fig. S2F). The role of VacA was then further investigated in macrophages cells infected with the *H. pylori* 26695 strain and the isogenic Δ*vacA* mutant [33], respectively. Immunoblotting analysis showed that the induction of NLRP3, pro-IL-1β and its matured cleavage was diminished in THP1 cells infected with *H. pylori* Δ*vacA* mutant (Fig. 2I). These data suggested that VacA is required for *H. pylori*-induced NLRP3 inflammasome activation.

To validate our findings in vivo, we infected the hypergastrinemic INS-GAS mice with *H. pylori* strain PMSS1, a widely used experimental animal model for *H. pylori* biology research. Colonization of *H. pylori* was confirmed by Warthin-Starry silver staining and CFU evaluation (Fig. S2G and H). Moreover, we observed increased levels of *H. pylori* specific serum IgG in *H. pylori*-infected mice compared to controls (Fig. S2I). H&E and AB-PAS staining showed that *H. pylori*-infected INS-GAS mice developed pathologic changes with severe inflammation and increased gastric metaplasia (Fig. 3A). The pathological subfeature scores in gastric tissues of infected mice were significantly higher than in control group (Fig. 3B, Table S4). The production of TNF-α and IL-1β were also elevated in serum from mice after *H. pylori* infection (Fig. 3C). Compared with control mice, the protein levels of TNFα, NLRP3, pro-IL-1β and cleaved caspase-1 were increased in the gastric tissues of *H. pylori*-infected mice (Fig. 3D). Immunofluorescence revealed that *H. pylori* infection induced the colocalization of CD68 and NLRP3 in the gastric tissues of INS-GAS mice (Fig. 3E). Taken together, these findings indicated with *H. pylori* induced NLRP3 inflammasome activation in macrophages in vitro and in vivo.

NLRP3 regulates *H. pylori*-induced M1 macrophage polarization

Upon *H. pylori* infection, macrophages polarize towards the M1 phenotype by production of pro-inflammatory cytokines [15]. Based on our finding regarding the potentially important role of NLRP3 in *H. pylori*-induced gastritis as above-described, we postulated that NLRP3 inflammasome activation is involved in M1 macrophage activation. We first sought to directly assess the effect of *H. pylori* on the change of macrophage phenotypes using THP1 cells as a cell model. The RT-PCR analysis revealed that the mRNA expression levels of pro-inflammatory cytokines, including *TNFα*, *IL-1β*, *IL-6*, *CCL2* and *CCL3*, were significantly increased after *H. pylori* infection, peaking at 24 h post-infection (Fig. S3A) and in a dose-dependent manner (Fig. S3B). Then we determined the change of macrophage phenotypes in vivo following infection with PMSS1 *H. pylori* strain. As expected, there was a significant induction of iNOS-expressing $CD68^+$M1 macrophages (Fig. S3C).

To investigate the role of NLRP3 in the macrophage polarization in response to *H. pylori* infection, the BMDMs was isolated from WT and *Nlrp3*-KO mice (Fig. S4B). Genotyping was conducted to verify the successful construction of *Nlrp3*-KO mice (Fig. S4A). The efficiency of the differentiation of BMDMs was confirmed by examining the expression of macrophage surface antigen F4/80 (Fig. S4C). The qRT-PCR analysis validated the differentiation efficiency in *Nlrp3*-deficient BMDMs (Fig. S4D). Western blot analysis further demonstrated that knockout of *Nlrp3* significantly abrogated *H. pylori*-induced inflammasome and reduced the maturation of inflammatory cytokine IL-1β (Fig. 4A and Fig. S4E). In addition, *H. pylori* infection induced the protein levels of IL-1β in supernatant of WT BMDMs, while it was decreased after knockout of *Nlrp3* (Fig. 4B). Furthermore, we found that several M1 macrophage markers, such as *TNF-α*, *IL-1β*, *IL6* and *CCL2*, were significantly downregulated in *H. pylori*-infected *Nlrp3*-deficient BMDMs (Fig. 4C). We

(See figure on next page.)

Fig. 2 *H. pylori* infection promotes NLRP3 inflammasome activation in macrophages. **A**, **B** ELISA for human IL-1β secretion in the supernatant of PMA-induced differentiated THP1 cells following infection with *H. pylori* PMSS1 strain at different MOI (**A**) or different time points (**B**). Data are expressed as the means ± SDs. **C** ELISA for IL-18 concentration in THP1 cells cocultured with *H. pylori* PMSS1 or NCTC11637 strain. **D**, **E** Western blots for NLRP3 inflammasome at different MOI after co-culture of THP1 cells with *H. pylori* PMSS1 (**D**) or NCTC11637 (**E**) strain. **F** Western blots for NLRP3 inflammasome-related proteins in THP1 cells infected with PMSS1 or NCTC11637 strain at indicated time points. **G** Immunofluorescence staining for NLRP3 (green) in THP1 cells following *H. pylori* infection for 24 h. Scale bar, 10 μm. **H** Representative immunofluorescence images (left panel) and quantification (right panel) of ASC speck formation after stimulation of THP1 cells with *H. pylori*. Scale bar, 10 μm. **I** Representative images (upper panel) and quantitative densitometric analysis (lower panel) of western blots for NLRP3 inflammasome proteins in THP1 cells infected with 26,695 and its VacA knockout mutant strain for 24 h.*, $P < 0.05$; **, $P < 0.01$; ***, $P < 0.001$

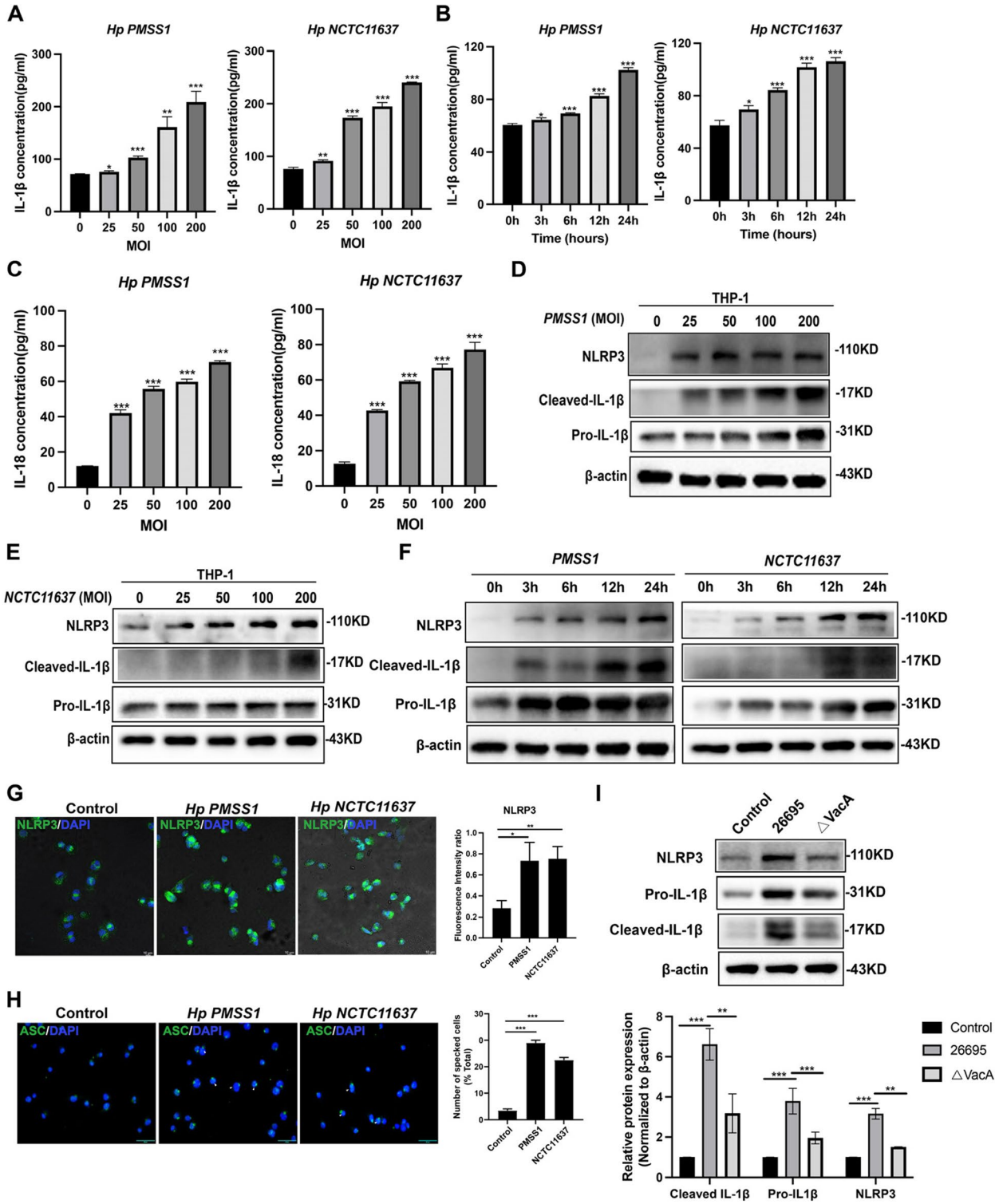

Fig. 2 (See legend on previous page.)

also confirmed these findings using the THP1 cells that were transfected with NLRP3 siRNA and then cocultured with *H. pylori*. Consistently, knockdown of NLRP3 by siRNA inhibited *H. pylori*-induced expression of pro-IL-β and cleaved IL-1β (Fig. 4D and Fig. S4F). And the IL-1β concentration was attenuated in the supernatant of

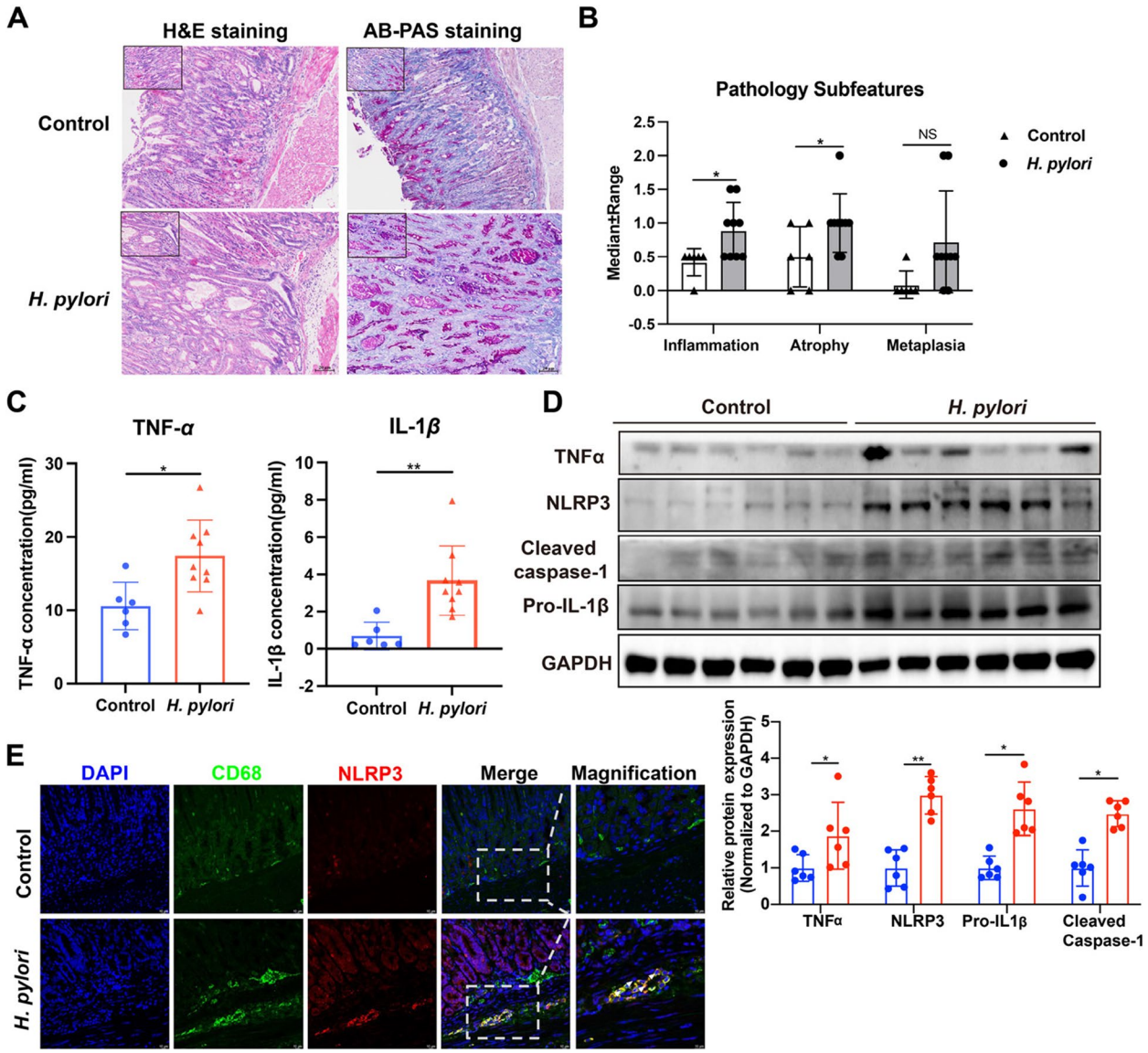

Fig. 3 *H. pylori* infection causes progressive gastritis and NLRP3 inflammasome activation in the gastric tissues of INS-GAS mice. **A** H&E and AB-PAS staining showing the histopathological features in gastric tissues of *H. pylori*-infected INS-GAS mice at 4 months post-infection. Scale bar, 20 μm. **B** The gastric inflammation, atrophy and metaplasia scores of categorical lesions in *H. pylori*-infected INS-GAS mice. Control group, $n = 6$; *H. pylori* group, $n = 9$. Each symbol is a different mouse. **C** ELISA assay showing the serum levels of TNFα and IL1β in *H. pylori*-infected INS-GAS mice at 4 months. **D** Western blots showing the expression of NLRP3 inflammasome-related proteins in gastric tissues of INS-GAS mice with or without *H. pylori* infection. Densitometric analysis of the immunoblots is depicted below. **E** Immunofluorescence staining for colocalization of CD68 and NLRP3 in gastric tissues of *H. pylori*-infected INS-GAS mice. Scale bar, 10 μm. The western blot results were representative of three independent experiments. The results were expressed as mean ± SEM of at least three independent experiments. *$P < 0.05$, **$P < 0.01$, ***$P < 0.001$, *NS, not significant*

THP1 cells following NLRP3 siRNA treatment (Fig. 4E). Knockdown of NLRP3 reduced the mRNA expression levels of M1 macrophage genes (Fig. 4F). As the NF-κB and STAT3 signaling pathway are well-known contributors to inflammatory response, we hypothesized that the NLRP3 inflammasome can regulate NF-κB and STAT3 activation. The western blot analysis indicated that *H. pylori* infection significantly induced STAT3 phosphorylation and IL-6 expression in WT BMDMs, while the induction was greatly ablated in the *Nlrp3*-deficient BMDMs (Fig. 4G and Fig. S4G). Of note, we found that NLRP3 knockout also suppressed *H. pylori*-induced NF-κB activation, shown by the reduced phosphorylated P65 levels (Fig. 4H and Fig. S4G). Similar findings were

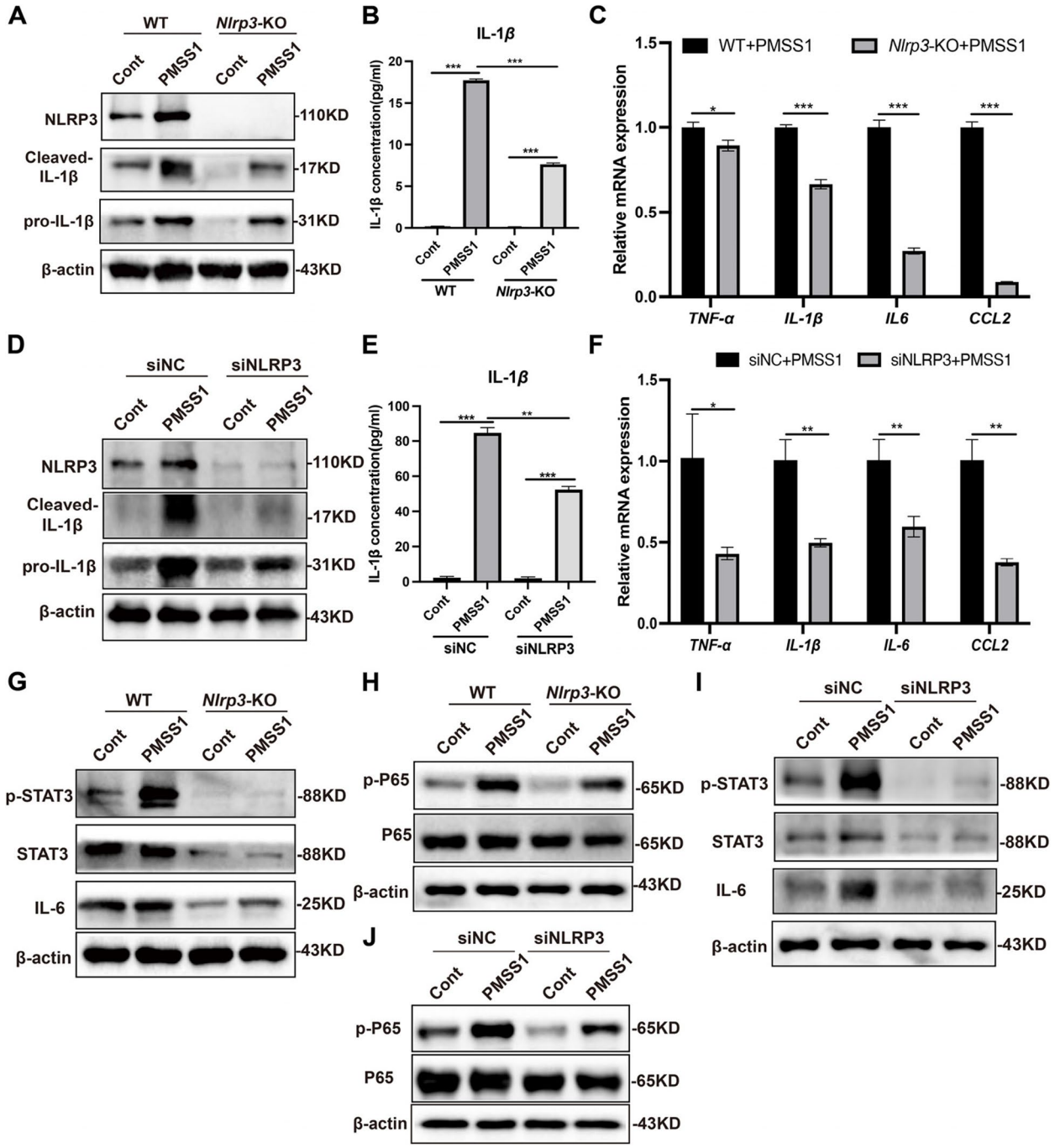

Fig. 4 NLRP3 is necessary for *H. pylori*-induced M1 macrophage polarization through the STAT3 and NF-κB pathways. **A** WT and *Nlrp3*-KO BMDMs were infected with *H. pylori* PMSS1 for 6 h. Western blot was performed to detect NLRP3 inflammasome proteins, such as NLRP3, Pro-IL-1β, and cleaved IL-1β, to confirm the efficiency of NLRP3 knockout. **B** IL1β concentration was determined by ELISA assay using the collected supernatant from the BMDMs treated in A. **C** WT and *Nlrp3*-KO BMDMs were infected with PMSS1, and the expression of M1 macrophage signature genes was measured by qRT-PCR. **D** & **E** THP1 cells were transfected with NLRP3 siRNA and then co-cultured with the PMSS1 strain. Western blotting was performed to detect the NLRP3 inflammasome protein levels (**D**). THP1 cell supernatant was collected for detection of IL-1β concentration by ELISA (**E**). **F** After the knockdown of NLRP3 and *H. pylori* PMSS1 strain treatment, M1 macrophage signature genes were measured by qRT-PCR. **G** and **H** WT and *Nlrp3*-KO BMDMs were infected with the PMSS1 strain for 6 h (**G**) and 1 h (**H**), respectively. Western blotting was performed to detect the proteins of STAT3 (**G**) and NF-κB pathways (**H**), respectively. **I** and **J** THP1 cells were transfected with NLRP3 siRNA and then infected with PMSS1 strain for 6 h (**I**) or 1 h (**J**). Western blotting analysis was performed to study the proteins of STAT3 (**I**) and NF-κB pathways (**J**), respectively. ** P < 0.05*, *** P < 0.01*, **** P < 0.001*

observed in THP1 cells, following treatment with NLRP3 siRNA and then infection with *H. pylori* PMSS1 strain (Fig. 4I-J and Fig. S4H). In summary, these results suggested that NLRP3 inflammasome promoted *H. pylori*-induced M1 macrophage polarization through activation of NF-κB and STAT3.

H. pylori activates NLRP3 inflammasome activation via TNFα

To further explore the underlying mechanism of NLRP3 activation, we compared the differential genes in cell populations with high and low NLRP3 expression in our previous scRNA-seq data [36]. The Kyoto Encyclopedia of Genes and Genomes (KEGG) enrichment analysis revealed that the TNF signaling pathway, which plays a crucial role in host immune and inflammation in response to *H. pylori* infection, is one of the most abundant pathways involved in NLRP3 activation (Fig. 5A). We then determined whether TNFα could activate NLRP3 inflammasome. Western blot analysis showed an increased in expression levels of NLRP3 and IL-1β levels following TNFα stimulation (Fig. 5B and Fig. S5A). The use of TNFα inhibitor QNZ [39], suppressed the TNFα-mediated increase in NLRP3, pro- and cleaved IL-1β protein levels (Fig. 5C and Fig. S5B). Of note, inhibition of TNF signaling by Atrosab [40], which typically inhibits TNFR1 binding to TNFα, also repressed NLRP3 inflammasome (Fig. 5D and Fig. S5C). In addition, qRT-PCR analysis showed that the expression of M1 macrophage marker genes, including *IL-1β*, *IL-6*, *CCL2* and *CCL3,* were upregulated upon TNFα stimulation, but at lower levels after treatment with TNF signaling inhibitor QNZ (Fig. 5E) or Atrosab (Fig. 5F).

Given the crucial role of TNFα in the activation of NLRP3 inflammasome, we hypothesized that TNFα is required for NLRP3 inflammasome activated by *H. pylori* infection. Indeed, from our scRNA-seq dataset [36], we found that TNF expression is significantly higher in human gastric tissues with *H. pylori* infection (15.21%) than in the uninfected individuals (10.84%) (Fig. 6A). Consistently, TNF was colocalized with CD68 and elevated in *H. pylori*-positive gastritis tissues compared to *H. pylori*-negative gastritis tissues (Fig. 6B). *H. pylori* infection increased the protein levels of TNF-α in THP1 cells with a trend in a MOI-dependent manner, however, this increase was not time-dependent (Fig. 6C and Fig. S6A-B). The concentration of TNF-α in the cell supernatant was also upregulated following *H. pylori* infection (Fig. 6D). Because our data indicated that the virulence factor plays an important role in *H. pylori*-induced NLRP3 inflammasome (Fig. 2I), we sought to determine whether VacA might be important for *H. pylori* infection-dependent TNF-α activation. We found that compared to the WT *H. pylori* strain, infection with the VacA-knockout mutant strain resulted in a significantly decreased expression of TNF-α (Fig. 6E). We further used TNF-α inhibitor to investigate whether *H. pylori* infection activated NLRP3 in a TNF-α-dependent manner. As expected, *H. pylori* infection-induced activation of NLRP3 inflammasome was abolished by treatment of TNF-α inhibitor QNZ (Fig. 6F and Fig. S6C) or Atrosab (Fig. 6G and Fig. S6D). Furthermore, inhibition of TNF-α downregulated the mRNA levels of M1 macrophage markers, such as *IL-1β*, *IL-6*, *CCL2* and *CCL3* (Fig. 6H-I). In summary, these data show that *H. pylori* infection triggers TNFα-regulated NLRP3 inflammasome activation and M1 macrophage polarization.

TNF/TNFR1 axis regulates NLRP3 inflammasome activation in *H. pylori*-infected macrophage

Using a recently established tool named CellChat [37], we inferred and compared cell–cell communication networks between *H. pylori*-positive and -negative gastric tissues, from our local scRNA-seq dataset. TNF signaling pathway network was identified as one of the most significant signaling pathways in *H. pylori*-positive gastric tissues (Fig. 7A). The heatmap plot further illustrates the activity of cellular signaling pathway networks across different cell types. As a result, TNF signaling network exhibits high activity in T and myeloid cells (Fig. 7B). The classical signaling pathway is transmitted through the binding of soluble TNF-α to TNFR1 or TNFR2. The proinflammatory function of TNF is dependent solely on TNFR1 signaling, which indeed contributes more to the TNF network in our dataset (Fig. S7A). These results raised a possibility that *H. pylori* infection activates

(See figure on next page.)

Fig. 5 TNFα stimulates NLRP3 inflammasome activation in macrophages. **A** KEGG pathway enrichment analysis was performed using the upregulated genes in NLRP3^{high} macrophages, in comparison with the NLRP3^{low} macrophages, according to our previous scRNA data of human gastric tissues. The dotted red box marked the enriched TNF signaling pathway. **B** Western blots showing the levels of NLRP3 inflammasome-related proteins in THP1 cells treated with different concentrations of TNF-α (0, 100, 200, and 400 ng/ml). **C** Western blots displaying the expression of NLRP3 inflammasome proteins in THP1 cells treated with TNF-α (200 ng/ml) in combination with TNFα inhibitor QNZ (400 ng/ml). **D** Western blots presenting the levels of NLRP3 inflammasome-related proteins in THP1 cells treated with TNF-α (200 ng/ml) in combination with TNFR1 antagonist Atrosab (1 μM). **E** and **F** qRT-PCR analysis of marker genes for M1 macrophages, including *TNF-α*, *IL-1β*, *IL-6*, *CCL2*, and *CCL3*, in THP1 cells, following stimulation with TNF and TNFα inhibitor QNZ (**E**), or with TNF and TNFR1 antagonist Atrosab (**F**). *$P < 0.05$, **$P < 0.01$, ***$P < 0.001$

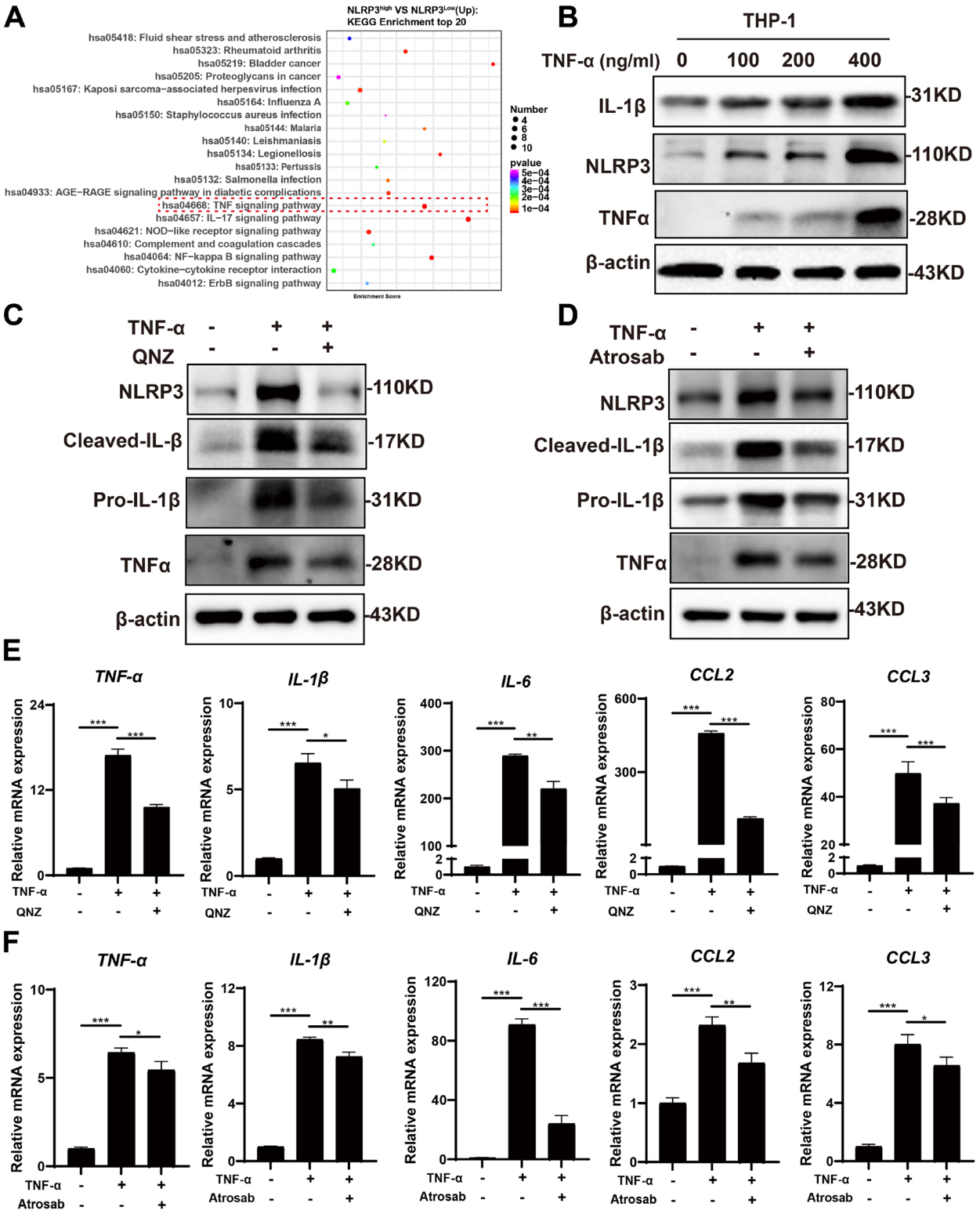

Fig. 5 (See legend on previous page.)

NLRP3 inflammasome through the TNF/TNFR1 axis. To identify the role of TNFR1 in NLRP3 inflammasome activation, we isolated BMDMs from WT and *Tnfr1* knockout mice and confirmed the efficiency of *Tnfr1* knockout by qRT-PCR analysis (Fig. S7B, C). To further validate the effect of TNF/TNFR1 axis on NLRP3 inflammasome in macrophage, BMDMs from WT or *Tnfr1*-KO mice were stimulated with TNF-α. The western blot analysis showed that NLRP3, pro-IL-1β and cleaved-IL-1β were significantly increased upon TNF-α treatment. However, their expression was lower in *Tnfr1*-KO BMDMs (Fig. S7D, E). In addition, there was a similar reduction in protein concentration of IL-1β in *Tnfr1*-deficicent BMDMs (Fig. S7F). We further investigated the NLRP3 inflammasome-related genes in WT and *Tnfr1*-deficient mice in the absence and presence of *H. pylori*. *H. pylori* infection led to upregulation of NLRP3, pro-IL-1β and cleaved-IL-1β protein levels (Fig. 7C and Fig. S7G), and increased the production of IL-1β (Fig. 7D). This induction was abolished in *H. pylori*-infected *Tnfr1*-deficient macrophages (Fig. 7C, D). Of note, the expression of M1 macrophage genes measured by qRT-PCR, including TNFα, IL-1β, IL-6, CCL2 and CCL3, were upregulated by TNFα treatment or *H. pylori* infection in WT BMDMs, but at lower levels in *Tnfr1*-knockout macrophages (Fig. 7E). Collectively, these data suggested that the TNF/TNFR1 axis is required for NLRP3 inflammasome activation in *H. pylori*-infected macrophages.

Discussion

Macrophages are the critical mediators in the innate immune response for host defense against many pathogens [41]. Polarization of gastric macrophages to M1 phenotype, which is characterized by production of pro-inflammatory cytokines, plays a crucial role in *H. pylori*-induced gastritis [15]. In this study, we determined NLRP3 as a key regulator of M1 macrophage polarization in response to *H. pylori* infection. In vivo and in vitro studies demonstrated that *H. pylori* infection promoted M1 macrophage activation and gastric inflammation by activating NLRP3 inflammasome by both in vivo and in vitro studies. Furthermore, we showed that the TNF/TNFR1 signaling axis regulated the NLRP3 inflammasome activation in *H. pylori*-infected macrophages. Our findings provide a novel link between *H. pylori* infection, TNF/TNFR signaling, NLRP3 inflammasome, M1 macrophage and gastritis (Fig. 7H).

NLRP3 inflammasome is associated with a wide range of diseases, such as inflammatory bowel diseases, cardiovascular diseases, arthritis, and cancer [18, 42, 43]. The assembly of the NLRP3 inflammasome complex triggers the maturation and secretion of pro-inflammatory cytokine IL-1β [44]. Several studies have indicated the activation of NLRP3 inflammasome in response to *H. pylori* infection, using different cell lines, such as gastric epithelial cells, T cells and macrophages [45–47]. Intriguingly, we found that NLRP3 is primarily expressed in myeloid cells (macrophages, monocytes, etc.) from our local scRNA-seq analysis of human gastric tissues [36]. We further validated the colocalization of CD68 (macrophage marker) and NLRP3, which was significantly increased in *H. pylori*-infected human gastritis tissues and stomach tissues of INS-GAS mice. Using cultured primary BMDMs from *Nlrp3*-deficient mice, we showed that knockout of *Nlrp3* remarkably inhibited M1 macrophage polarization and pro-inflammatory cytokines production induced by *H. pylori*. These findings suggested the crucial role of NLRP3 inflammasome activation in M1 macrophage during *H. pylori* infection-triggered gastritis. Our findings are in agreement with previous studies indicating that *H. pylori* infection induces NLRP3 inflammasome in the monocytes THP1 cell line [48]. Notably, we found that the PMSS1 strain lacking CagA was still capable of inducing NLRP3 inflammasome, while the *H. pylori* mutant lacking the toxin VacA resulted in lower levels of NLPR3 and IL-1β. These findings align with previous observation by Semper. et al. showing that the secretion of IL-1β induced by *H. pylori* was primarily regulated by the virulence factors VacA and CagPAI, rather than CagA [49]. Based on these data, we suggest that NLRP3 inflammasome activation is responsible for M1 macrophage phenotype and gastritis during *H. pylori* infection.

(See figure on next page.)

Fig. 6 *H. pylori* induces NLRP3 inflammasome and promotes M1 macrophage polarization through TNFα. **A** The UMAP plots indicated TNF expression in human gastric tissues from our scRNA-seq data. **B** Immunofluorescence staining for the co-expression of CD68 (green) and TNFα (red) in human gastritis tissues with or without *H. pylori* infection. Scale bar, 10 μm. **C** Western blot assay for TNFα protein expression in THP1 cells infected with *H. pylori* at various MOIs for 24 h (upper panel), or treated with *H. pylori* at an MOI of 100 for indicated time points (lower panel). **D** ELISA assay for detection of the TNF-α concentration in the supernatant of THP1 cells following *H. pylori* infection with indicated MOI (left panel) or at indicated time points (right panel). **E** Western blots for the TNFα expression in THP1 cells infected with *H. pylori* 26,695 strain or its VacA^{-} mutant. **F** and **G** Western blots for the protein expression of NLRP3 inflammasome in THP1 cells treated with TNF-α in combination with TNFα inhibitor QNZ (**F**), or in combination with TNFR1 antagonist Atrosab (**G**). **H** and **I** The qRT-PCR analysis of mRNA levels of M1 macrophage signature genes in THP1 cells treated with TNF-α in combination with QNZ (**H**), or in combination with Atrosab (**I**). *$P < 0.05$, **$P < 0.01$

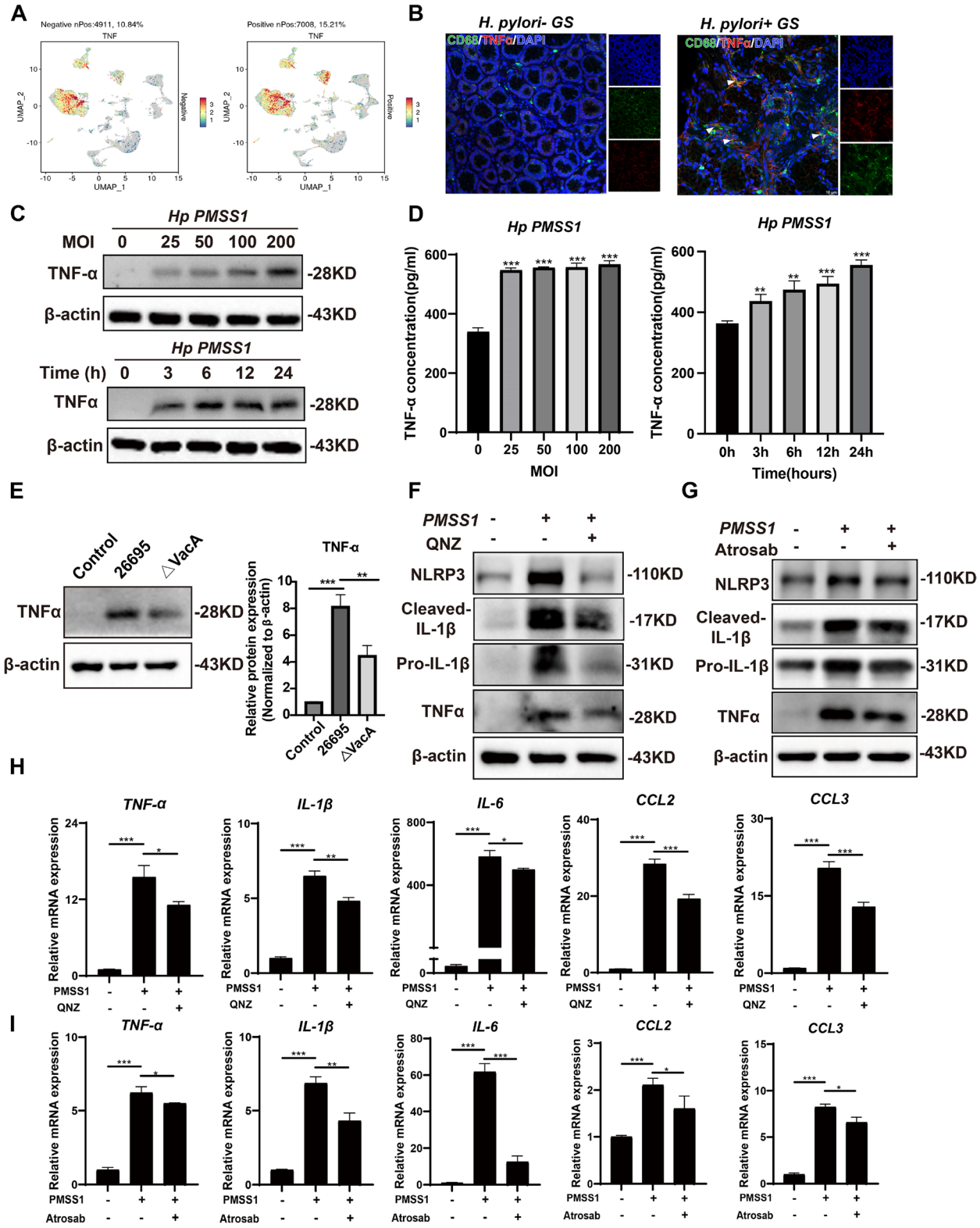

Fig. 6 (See legend on previous page.)

It has been reported that *H. pylori* infection causes TNFα production in gastric epithelial cells and macrophages [50–52]. Several studies have highlighted the importance of TNF in the clinical progression of *H. pylori* infection. TNF exerts its biological functions, such as pro-inflammatory activity, cell proliferation, survival and apoptosis, by binding to either TNFR1 or TNFR2 [27]. However, the role of the TNF/TNFR1 signaling pathway in the pathogenesis of *H. pylori* is still poorly understood. A previous study [53] has indicated the crucial role of TNFα and TNFR1 in BMDMs in gastric tumorigenesis using genetic mouse models. The development of gastric tumors was significantly suppressed in *Gan* mice with TNFR1 or TNF deficiency. Transplantation of BMDMs from *Tnfr1*-KO mice to WT mice resulted in a reduction of gastric tumor growth [53]. In this study, we observed elevated levels of TNF in human gastric tissues infected with *H. pylori* compared to uninfected tissues.

Consistent with the role of TNF in the proinflammatory response, we found that a selective inhibitor of TNF, QNZ, significantly blocked the polarization of M1 macrophage induced by *H. pylori*. Furthermore, as a TNFR1 antagonist, Atrosab selectively blocks TNFR1, without affecting TNFR2, and was shown to exert potential therapeutic effects in chronic inflammatory diseases [54]. Here, we demonstrated that Atrosab was also capable of suppressing *H. pylori*-induced M1 macrophage polarization. Therefore, we propose the crucial role of TNF/TNFR1 signaling in *H. pylori* infection-induced macrophage activation and gastric inflammation. TNF inhibitors have been widely used to treat various inflammatory diseases, such as rheumatoid arthritis, psoriatic arthritis and inflammatory bowel disease (IBD) [55–57]. Our findings suggest the TNF inhibitors as potential candidates for the treatment of *H. pylori*-associated gastric disorders.

Activation of NLRP3 inflammasome triggers IL-1β maturation through two steps: first, the priming step which is required for increased expression of NLRP3, and the activation step that leads to inflammasome formation [58]. The priming process of inflammasome is triggered by pattern recognition receptor signaling, e.g., TLRs, which subsequently promotes the NF-κB signaling pathway, leading to NLRP3 activation and IL-1β maturation [59]. A previous study reported that TLR2 is responsible for *H. pylori*-induced NLRP3 inflammasome and thereby production of regulatory T cells [45]. Our findings demonstrated the specific role of the TNF/TNFR signaling axis in the activation of NLRP3 inflammasome in macrophages upon *H. pylori* infection. Of note, we found that TNFR1 is essential for NLRP3 inflammasome activation in response to *H. pylori* infection. BMDMS isolated from *Tnfr1*-KO mice expressed lower levels of NLRP3 and IL-1β following *H. pylori* infection, when compared with WT BMDMs, in line with a previous study showing that TNFα is a transcriptional regulator of NLRP3 inflammasome components in murine inflammatory diseases [60]. In addition, various molecular or cellular events are linked to NLRP3 inflammasome activation, including K^+ efflux, Ca^{2+} signaling, mitochondrial dysfunction and ROS [58]. It is widely known that *H. pylori* damage induces mitochondrial dysfunction and ROS accumulation, which might be closely related to NLRP3 inflammasome [61].

There are several limitations of the study. Macrophages are not the primary contact with *H. pylori* in the tissue. The present study employs a model of macrophage infection with high MOI of *H. pylori* bacteria, despite considerable supporting evidence. Nonetheless, this approach may not entirely reflect the actual situation. Additionally, we did not have antibiotic selective plates working for negative control experiments.

(See figure on next page.)

Fig. 7 TNF/TNFR1 axis is responsible for *H. pylori*-induced NLRP3 inflammasome activation and M1 macrophage activation. **A**, **B** CellChat analysis was used to identify cell–cell communication signaling network between *H. pylori*-positive and *H. pylori*-negative gastritis tissues. CellChat calculates communication probabilities at the signaling pathway by summarizing all ligand-receptor interactions associated with each signaling pathway. If the ratio of the total pathway probabilities between the comparison group and the control group is < 0.95 and *p*-value < 0.05, the communication strength in the control group was considered as significant (y-axis in red); whereas if the total ratio is > 1.05 and *p*-value < 0.05, the communication strength in the comparison group was considered as significant (y-axis in blue). *H. pylori*-positive tissues as the comparison group; *H. pylori*-negative tissues as control group. **A** The bar charts showed the most significant differential signaling pathways. The dotted red box highlighted TNF signaling as the top upregulated pathway in *H. pylori*-positive gastritis tissues, compared to *H. pylori*-negative tissues. **B** The heatmap plot showing differential cellular communication networks among different cell populations in *H. pylori*-positive and -negative gastritis tissues. The TNF signaling network was highlighted with a red box. **C** WT and *Tnfr1*-KO BMDMs were infected with *H. pylori* PMSS1 strain (MOI = 100). Western blots for the protein expression of molecules of NLRP3 inflammasome. **D** ELISA for IL-1β concentration in cell supernatant. **E** The qRT-PCR analysis for M1 macrophage signature genes expression in TNFα or PMSS1-treated BMDMs from WT and *Tnfr1*-deficient mice. **F** The working model of the TNF/TNFR1 axis-mediated activation of NLRP3 inflammasome in macrophages and M1 polarization during *H. pylori* infection. *H. pylori* infection induces the production of TNFα, which binds to TNFR1, promoting the NLRP3 inflammasome activation in macrophages, and resulting in M1 macrophage polarization and gastric inflammation through activation of NF-κB and STAT3 signaling pathways

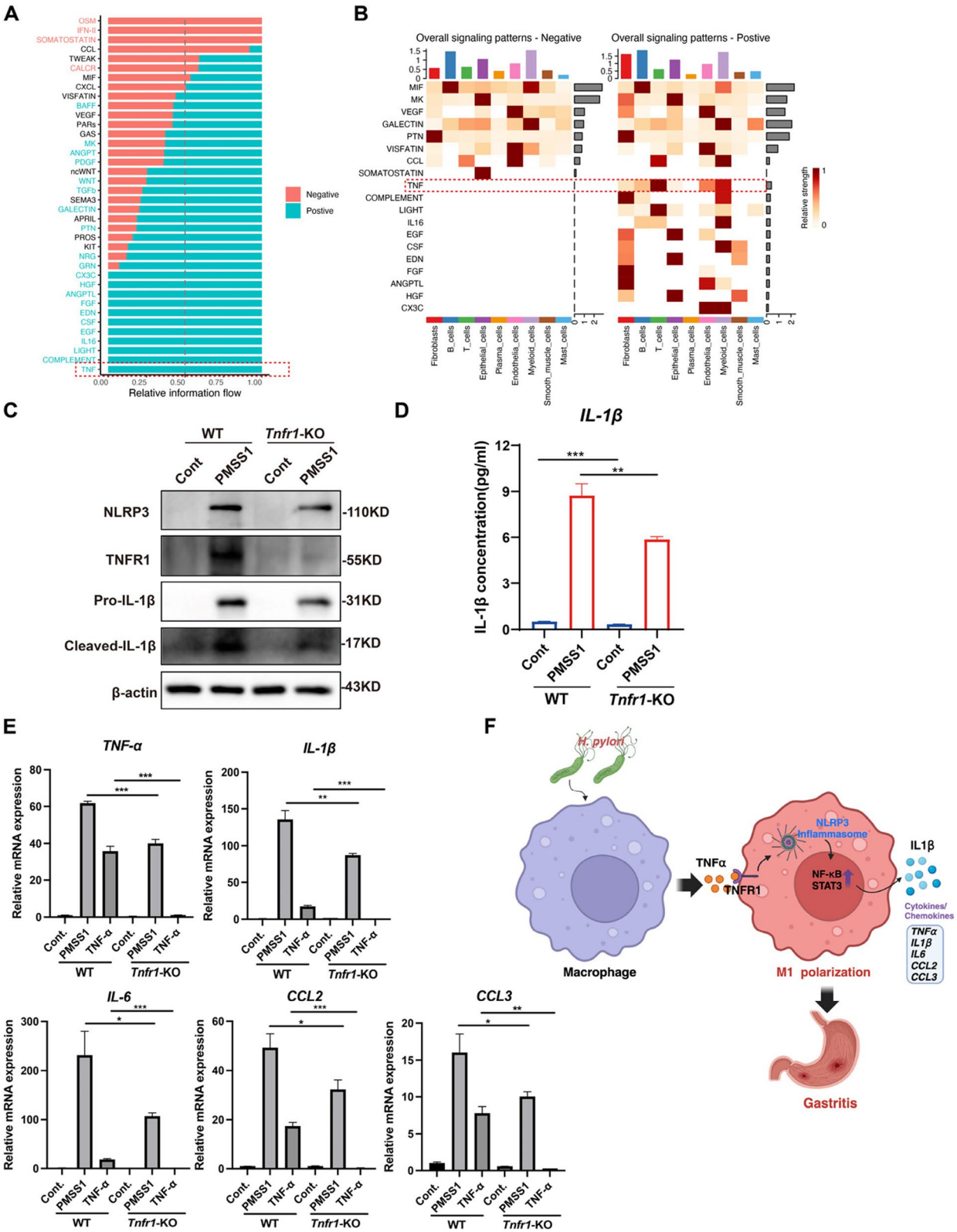

Fig. 7 (See legend on previous page.)

In summary, this study presents a novel mechanism by which *H. pylori* activates NLRP3 inflammasome through the TNF/TNFR1 signaling, thereby inducing M1 macrophage polarization and gastritis. Our results further confirmed that NLRP3 is specifically expressed in macrophage from gastric tissues. This might provide an explanation for why it plays such a significant role in M1 macrophage activation and gastric inflammation in response to *H. pylori* infection. Furthermore, the use of inhibitors of the TNF/TNFR1 signaling axis or knockout of *Tnfr1* to block the TNF/TNFR1 signaling significantly attenuated NLRP3 inflammasome activation induced by *H. pylori*. Although it remains still unclear whether NLRP3 deficiency in experimental models can improve gastric pathology caused by *H. pylori* infection, our findings suggest that inhibition of TNF signaling and NLRP3 inflammasome could be a viable approach to manage excessive gastric inflammation and damage induced by *H. pylori* infection.

Supplementary Information

The online version contains supplementary material available at https://doi.org/10.1186/s12964-024-02017-7.

Supplementary Material 1.

Supplementary Material 2.

Supplementary Material 3.

Supplementary Material 4.

Supplementary Material 5.

Supplementary Material 6.

Acknowledgements
We thank Prof. Chunhui Lan from Daping Hospital of the Third Military Medical University for providing H. pylori strain 26695 and its VacA- mutant.

Authors' contributions
XF, NSL, and YZ conceived and designed the study. XF, SHC, and NSL performed in vitro experiments and analyzed the data. XF, XBX, LYL and HJK collected human specimens and analyzed immunohistochemical data. HW and XDW performed animal studies. CH, CX, JPL and YX assisted with data analyses. XF, NSL, YZ and JPL interpreted the data and drafted the manuscript. NSL and YZ supervised and oversaw the study. All authors revised the manuscript, provided intellectual content, and approved the final manuscript.

Funding
This work was supported by the Academic and Technical Leader of major disciplines in Jiangxi Province (20225BCJ23021), Natural Science Foundation of Jiangxi Province (20224ACB216004), National Natural Science Foundation of China (82260119, 82170580 and 81870395), Chunhui Program of the Ministry of Education (HZKY20220394), Jiangxi Provincial Health Commission project (202410013), and the Key Laboratory Project of Digestive Diseases in Jiangxi Province (2024SSY06101).

Data availability
No datasets were generated or analysed during the current study.

Declarations

Ethics approval and consent to participate
All experimental procedures were conducted according to the guidelines approved by the Ethics Committee (2023CDYFYYLK01-09) and Animal Ethics Committee (CDYFY-IACUC-202302QR004) of the First Affiliated Hospital of Nanchang University.

Consent for publication
Not applicable.

Competing interests
The authors declare no competing interests.

Author details
[1]Department of Gastroenterology, Jiangxi Provincial Key Laboratory of Digestive Diseases, Jiangxi Clinical Research Center for Gastroenterology, Digestive Disease Hospital, The First Affiliated Hospital, Jiangxi Medical College, Nanchang University, Nanchang, Jiangxi, China. [2]Postdoctoral Innovation Practice Base, The First Affiliated Hospital, Jiangxi Medical College, Nanchang University, Nanchang, China. [3]Department of Drug Safety Evaluation, Jiangxi Testing Center of Medical Instruments, Nanchang, China.

Received: 6 August 2024 Accepted: 27 December 2024
Published online: 06 January 2025

References

1. Malfertheiner P, Camargo MC, El-Omar E, Liou JM, Peek R, Schulz C, Smith SI, Suerbaum S. Helicobacter pylori infection. Nat Rev Dis Primers. 2023;9(1):19.
2. Crowe SE. Helicobacter pylori Infection. N Engl J Med. 2019;380(12):1158–65.
3. Chen YC, Malfertheiner P, Yu HT, Kuo CL, Chang YY, Meng FT, Wu YX, Hsiao JL, Chen MJ, Lin KP, et al. Global prevalence of helicobacter pylori infection and incidence of gastric cancer between 1980 and 2022. Gastroenterology. 2024;166(4):605–19.
4. Malfertheiner P, Megraud F, Rokkas T, Gisbert JP, Liou JM, Schulz C, Gasbarrini A, Hunt RH, Leja M, O'Morain C, et al. Management of helicobacter pylori infection: the Maastricht VI/Florence consensus report. Gut. 2022;71:1724–62.
5. Correa P, Piazuelo MB. Helicobacter pylori infection and gastric adenocarcinoma. US Gastroenterol Hepatol Rev. 2011;7(1):59–64.
6. Li N, Xu X, Zhan Y, Fei X, Ouyang Y, Zheng P, Zhou Y, He C, Xie C, Hu Y, et al. YAP and beta-catenin cooperate to drive H. pylori-induced gastric tumorigenesis. Gut Microbes. 2023;15(1):2192501.
7. Polk DB, Peek RM Jr. Helicobacter pylori: gastric cancer and beyond. Nat Rev Cancer. 2010;10(6):403–14.
8. Yan L, Chen Y, Chen F, Tao T, Hu Z, Wang J, You J, Wong BCY, Chen J, Ye W. Effect of helicobacter pylori eradication on gastric cancer prevention: updated report from a randomized controlled trial with 26.5 years of follow-up. Gastroenterology. 2022;163:154-162.e3.
9. Chiang TH, Chang WJ, Chen SL, Yen AM, Fann JC, Chiu SY, Chen YR, Chuang SL, Shieh CF, Liu CY, et al. Mass eradication of Helicobacter pylori to reduce gastric cancer incidence and mortality: a long-term cohort study on Matsu Islands. Gut. 2021;70(2):243–50.
10. Moss SF, Shah SC, Tan MC, El-Serag HB. Evolving concepts in helicobacter pylori management. Gastroenterology. 2024;166(2):267–83.
11 Blosse A, Lehours P, Wilson KT, Gobert AP. Helicobacter: Inflammation, immunology, and vaccines. Helicobacter. 2018;23 Suppl 1(Suppl 1):e12517.
12. Locati M, Curtale G, Mantovani A. Diversity, mechanisms, and significance of macrophage plasticity. Annu Rev Pathol. 2020;15:123–47.
13. Wynn TA, Chawla A, Pollard JW. Macrophage biology in development, homeostasis and disease. Nature. 2013;496(7446):445–55.
14. Hardbower DM, Asim M, Luis PB, Singh K, Barry DP, Yang C, Steeves MA, Cleveland JL, Schneider C, Piazuelo MB, et al. Ornithine decarboxylase regulates M1 macrophage activation and mucosal inflammation via histone modifications. Proc Natl Acad Sci U S A. 2017;114(5):E751–60.

15. Modi N, Chen Y, Dong X, Hu X, Lau GW, Wilson KT, Peek RM Jr, Chen LF. BRD4 regulates glycolysis-dependent Nos2 expression in macrophages upon H pylori infection. Cell Mol Gastroenterol Hepatol. 2024;17(2):292-308 e291.
16. Kaparakis M, Walduck AK, Price JD, Pedersen JS, van Rooijen N, Pearse MJ, Wijburg OL, Strugnell RA. Macrophages are mediators of gastritis in acute Helicobacter pylori infection in C57BL/6 mice. Infect Immun. 2008;76(5):2235–9.
17. Fu J, Wu H. Structural mechanisms of NLRP3 inflammasome assembly and activation. Annu Rev Immunol. 2023;41:301–16.
18. Swanson KV, Deng M, Ting JP. The NLRP3 inflammasome: molecular activation and regulation to therapeutics. Nat Rev Immunol. 2019;19(8):477–89.
19. VandeWalle L, Lamkanfi M. Drugging the NLRP3 inflammasome: from signalling mechanisms to therapeutic targets. Nat Rev Drug Discov. 2024;23(1):43–66.
20. Li X, He C, Li N, Ding L, Chen H, Wan J, Yang X, Xia L, He W, Xiong H, et al. The interplay between the gut microbiota and NLRP3 activation affects the severity of acute pancreatitis in mice. Gut Microbes. 2020;11(6):1774–89.
21. Wang X, Eagen WJ, Lee JC. Orchestration of human macrophage NLRP3 inflammasome activation by Staphylococcus aureus extracellular vesicles. Proc Natl Acad Sci U S A. 2020;117(6):3174–84.
22. Tsukalov I, Sanchez-Cerrillo I, Rajas O, Avalos E, Iturricastillo G, Esparcia L, Buzon MJ, Genesca M, Scagnetti C, Popova O, et al. NFkappaB and NLRP3/NLRC4 inflammasomes regulate differentiation, activation and functional properties of monocytes in response to distinct SARS-CoV-2 proteins. Nat Commun. 2024;15(1):2100.
23. Choi HR, Lim H, Lee JH, Park H, Kim HP. Interruption of Helicobacter pylori-Induced NLRP3 Inflammasome activation by chalcone derivatives. Biomol Ther (Seoul). 2021;29(4):410–8.
24. Perez-Figueroa E, Torres J, Sanchez-Zauco N, Contreras-Ramos A, Alvarez-Arellano L, Maldonado-Bernal C. Activation of NLRP3 inflammasome in human neutrophils by Helicobacter pylori infection. Innate Immun. 2016;22(2):103–12.
25. Zhang X, Li C, Chen D, He X, Zhao Y, Bao L, Wang Q, Zhou J, Xie YH. pylori CagA activates the NLRP3 inflammasome to promote gastric cancer cell migration and invasion. Inflamm Res. 2022;71(1):141–55.
26. Soraci L, Gambuzza ME, Biscetti L, Lagana P, Lo Russo C, Buda A, Barresi G, Corsonello A, Lattanzio F, Lorello G, et al. Toll-like receptors and NLRP3 inflammasome-dependent pathways in Parkinson's disease: mechanisms and therapeutic implications. J Neurol. 2023;270(3):1346–60.
27. van Loo G, Bertrand MJM. Death by TNF: a road to inflammation. Nat Rev Immunol. 2023;23(5):289–303.
28. Dostert C, Grusdat M, Letellier E, Brenner D. The TNF family of ligands and receptors: communication modules in the immune system and beyond. Physiol Rev. 2019;99(1):115–60.
29. Webster JD, Vucic D. The balance of TNF mediated pathways regulates inflammatory cell death signaling in healthy and diseased tissues. Front Cell Dev Biol. 2020;8:365.
30. Fischer R, Kontermann RE, Pfizenmaier K. Selective targeting of TNF receptors as a novel therapeutic approach. Front Cell Dev Biol. 2020;8:401.
31. Preedy MK, White MRH, Tergaonkar V. Cellular heterogeneity in TNF/TNFR1 signalling: live cell imaging of cell fate decisions in single cells. Cell Death Dis. 2024;15(3):202.
32. Ge Z, Sheh A, Feng Y, Muthupalani S, Ge L, Wang C, Kurnick S, Mannion A, Whary MT, Fox JG. Helicobacter pylori-infected C57BL/6 mice with different gastrointestinal microbiota have contrasting gastric pathology, microbial and host immune responses. Sci Rep. 2018;8(1):8014.
33. Xie C, Li N, Wang H, He C, Hu Y, Peng C, Ouyang Y, Wang D, Xie Y, Chen J, et al. Inhibition of autophagy aggravates DNA damage response and gastric tumorigenesis via Rad51 ubiquitination in response to H. pylori infection. Gut Microbes. 2020;11(6):1567–89.
34. Li N, Feng Y, Hu Y, He C, Xie C, Ouyang Y, Artim SC, Huang D, Zhu Y, Luo Z, et al. Helicobacter pylori CagA promotes epithelial mesenchymal transition in gastric carcinogenesis via triggering oncogenic YAP pathway. J Exp Clin Cancer Res. 2018;37(1):280.
35. Rogers AB, Taylor NS, Whary MT, Stefanich ED, Wang TC, Fox JG. Helicobacter pylori but not high salt induces gastric intraepithelial neoplasia in B6129 mice. Cancer Res. 2005;65(23):10709–15.
36. Li N, Chen S, Xu X, Wang H, Zheng P, Fei X, Ke H, Lei Y, Zhou Y, Yang X, et al. Single-cell transcriptomic profiling uncovers cellular complexity and microenvironment in gastric tumorigenesis associated with Helicobacter pylori**.** J Adv Res. 2024. Available from: https://www.sciencedirect.com/science/article/pii/S2090123224004661?via%3Dihub.
37. Jin S, Plikus MV, Nie Q. CellChat for systematic analysis of cell-cell communication from single-cell transcriptomics**.** Nat Protoc. 2025;20:180–219.
38. Xu X, Shu C, Wu X, Ouyang Y, Cheng H, Zhou Y, Wang H, He C, Xie C, He X, et al. A positive feedback loop of the TAZ/beta-catenin axis promotes Helicobacter pylori-associated gastric carcinogenesis. Front Microbiol. 2022;13:1065462.
39. Al-Gayyar MMH, Alattar A, Alshaman R, Hamdan AM. QNZ alleviated hepatocellular carcinoma by targeting inflammatory pathways in a rat model. Cytokine. 2021;148:155710.
40. Zhang H, Shi N, Diao Z, Chen Y, Zhang Y. Therapeutic potential of TNFalpha inhibitors in chronic inflammatory disorders: Past and future. Genes Dis. 2021;8(1):38–47.
41. Chen S, Saeed A, Liu Q, Jiang Q, Xu H, Xiao GG, Rao L, Duo Y. Macrophages in immunoregulation and therapeutics. Signal Transduct Target Ther. 2023;8(1):207.
42. Toldo S, Mezzaroma E, Buckley LF, Potere N, Di Nisio M, Biondi-Zoccai G, Van Tassell BW, Abbate A. Targeting the NLRP3 inflammasome in cardiovascular diseases. Pharmacol Ther. 2022;236:108053.
43. Sharma BR, Kanneganti TD. NLRP3 inflammasome in cancer and metabolic diseases. Nat Immunol. 2021;22(5):550–9.
44. Paik S, Kim JK, Silwal P, Sasakawa C, Jo EK. An update on the regulatory mechanisms of NLRP3 inflammasome activation. Cell Mol Immunol. 2021;18(5):1141–60.
45. Koch KN, Muller A. Helicobacter pylori activates the TLR2/NLRP3/caspase-1/IL-18 axis to induce regulatory T-cells, establish persistent infection and promote tolerance to allergens. Gut Microbes. 2015;6(6):382–7.
46. Yu Q, Shi H, Ding Z, Wang Z, Yao H, Lin R. The E3 ubiquitin ligase TRIM31 attenuates NLRP3 inflammasome activation in Helicobacter pylori-associated gastritis by regulating ROS and autophagy. Cell Commun Signal. 2023;21(1):1.
47. Ng GZ, Menheniott TR, Every AL, Stent A, Judd LM, Chionh YT, Dhar P, Komen JC, Giraud AS, Wang TC, et al. The MUC1 mucin protects against Helicobacter pylori pathogenesis in mice by regulation of the NLRP3 inflammasome. Gut. 2016;65(7):1087–99.
48. Pachathundikandi SK, Blaser N, Bruns H, Backert S. Helicobacter pylori avoids the critical activation of NLRP3 inflammasome-mediated production of oncogenic mature IL-1beta in human immune cells. Cancers (Basel). 2020;12(4):803.
49. Semper RP, Mejias-Luque R, Gross C, Anderl F, Muller A, Vieth M, Busch DH, Prazeres da Costa C, Ruland J, Gross O, Gerhard M. Helicobacter pylori-induced IL-1beta secretion in innate immune cells is regulated by the NLRP3 inflammasome and requires the cag pathogenicity island. J Immunol. 2014;193(7):3566–76.
50. Tavares R, Pathak SK. Induction of TNF, CXCL8 and IL-1beta in macrophages by Helicobacter pylori secreted protein HP1173 occurs via MAP-kinases, NF-kappaB and AP-1 signaling pathways. Microb Pathog. 2018;125:295–305.
51. Malespin-Bendana W, Alpizar-Alpizar W, Figueroa-Protti L, Reyes L, Molina-Castro S, Une C, Ramirez-Mayorga V. Helicobacter pylori infection induces gastric precancerous lesions and persistent expression of Angpt2, Vegf-A and Tnf-A in a mouse model. Front Oncol. 2023;13:1072802.
52. Li T, Shao W, Li S, Ma L, Zheng L, Shang W, Jia X, Sun P, Liang X, Jia JH. pylori infection induced BMAL1 expression and rhythm disorder aggravate gastric inflammation. EBioMedicine. 2019;39:301–14.
53. Oshima H, Ishikawa T, Yoshida GJ, Naoi K, Maeda Y, Naka K, Ju X, Yamada Y, Minamoto T, Mukaida N, et al. TNF-alpha/TNFR1 signaling promotes gastric tumorigenesis through induction of Noxo1 and Gna14 in tumor cells. Oncogene. 2014;33(29):3820–9.
54. Richter F, Williams SK, John K, Huber C, Vaslin C, Zanker H, Fairless R, Pichi K, Marhenke S, Vogel A, et al. The TNFR1 antagonist atrosimab is therapeutic in mouse models of acute and chronic inflammation. Front Immunol. 2021;12:705485.

55. Kalden JR, Schulze-Koops H. Immunogenicity and loss of response to TNF inhibitors: implications for rheumatoid arthritis treatment. Nat Rev Rheumatol. 2017;13(12):707–18.
56. Cui G, Fan Q, Li Z, Goll R, Florholmen J. Evaluation of anti-TNF therapeutic response in patients with inflammatory bowel disease: current and novel biomarkers. EBioMedicine. 2021;66:103329.
57. Deodhar A, Helliwell PS, Boehncke WH, Kollmeier AP, Hsia EC, Subramanian RA, Xu XL, Sheng S, Agarwal P, Zhou B, et al. Guselkumab in patients with active psoriatic arthritis who were biologic-naive or had previously received TNFalpha inhibitor treatment (DISCOVER-1): a double-blind, randomised, placebo-controlled phase 3 trial. Lancet. 2020;395(10230):1115–25.
58. Akbal A, Dernst A, Lovotti M, Mangan MSJ, McManus RM, Latz E. How location and cellular signaling combine to activate the NLRP3 inflammasome. Cell Mol Immunol. 2022;19(11):1201–14.
59. Chen Y, Ye X, Escames G, Lei W, Zhang X, Li M, Jing T, Yao Y, Qiu Z, Wang Z, et al. The NLRP3 inflammasome: contributions to inflammation-related diseases. Cell Mol Biol Lett. 2023;28(1):51.
60. McGeough MD, Wree A, Inzaugarat ME, Haimovich A, Johnson CD, Pena CA, Goldbach-Mansky R, Broderick L, Feldstein AE, Hoffman HM. TNF regulates transcription of NLRP3 inflammasome components and inflammatory molecules in cryopyrinopathies. J Clin Invest. 2017;127(12):4488–97.
61 Sah DK, Arjunan A, Lee B, Jung YD. Reactive oxygen species and H. pylori infection: a comprehensive review of their roles in gastric cancer development. Antioxidants (Basel). 2023;12(9):1712.

Publisher's Note